Molecular Catalysis 550 (2023) 113613

Contents lists available at ScienceDirect

Molecular Catalysis

journal homepage: www.journals.elsevier.com/molecular-catalysis

Surface engineering of cyclodextrin glycosyltransferase reveals structural compactness and rigidity responsible for enhanced organic solvents resistance

Ruizhi Han [a,b,1,*], Yulin Jiang [a,1], Siyan Liu [a], Yu Ji [b], Ulrich Schwaneberg [b,c,*], Ye Ni [a]

[a] Key laboratory of Industrial Biotechnology, School of Biotechnology, Jiangnan University, Wuxi 214122, China
[b] Institute of Biotechnology, RWTH Aachen University, Aachen 52074, Germany
[c] DWI-Leibniz Institute for Interactive Materials, Aachen 52074, Germany

ARTICLE INFO

Keywords:
Cyclodextrin glycosyltransferase
Semi-rational design
Organic solvent resistance
Surface engineering
MD simulation

ABSTRACT

Cyclodextrin glycosyltransferase (CGTase) is a preferable biocatalyst for production of cyclodextrin and phenols glycosylated derivatives due to its cost-effective donors and broad range of acceptors. Organic solvents (OSs) are often beneficial for solubilizing hydrophobic substrates and product specificity, but often harmful towards CGTases. Herein, using *Paenibacillus macerans* CGTase (*Pm*CGTase) as a template and DMSO as a screening solvent, semi-rational engineering was performed at 18 surface residues by a developed high throughput screening method. Using site saturation mutagenesis and iterative saturation mutagenesis, 5 OSs-resistant variants (G539I, G539V, G539I/R146F, G539V/R146A, G539I/R146F/D147N) were obtained. Compared with WT, the best variant G539I/R146F/D147N showed a 79.3 % enhanced residual activity at 30 % DMSO and a 60 % increased $t_{1/2}$ value at both 40 and 50 °C. In addition, a decreased K_m value and an increased k_{cat} value led to 41.9 % higher catalytic efficiency of G539I/R146F/D147N than WT in 15 % DMSO. This variant was also applied to glycosylation of sophoricoside in 20 % DMSO, leading to 26.2 % increased conversion. Molecular dynamics demonstrates that its enhanced OSs resistance may be attributed to the strengthened structural compactness and rigidity. Our results provide guidance for engineering OSs resistance of *Pm*CGTase, which would further improve its application potential.

Introduction

Cyclodextrin glycosyltransferase (CGTase, EC 2.4.1.19) belongs to α-amylase family of glycosyl hydrolases (GH 13) [1]. CGTases mainly catalyze three types of transglycosylation reactions (cyclization, coupling, and disproportionation), leading to its wide applications in food and nourishment fields [2,3]. Commonly, CGTases can be used for cyclodextrin (CD) production [4–7]. In addition, CGTases are also used for the synthesis of high-value products by the transglycosylation. For instance, CGTases can catalyze the glycosylation of L-ascorbic acid (L-AA) for the synthesis of 2-*O*-glucopyranosyl-L-ascorbic acid (AA-2 G), which greatly improves its stability in water [8,9]. Flavonoids compounds (e.g., genistin [10,11], rutin [12], bioflavonoids [13]) can be glycosylated by CGTase to increase their solubility in water. In addition, glycosylation of stevioside by CGTases could alleviate its bitter taste [14,15].

Organic solvents (OSs) play a crucial role in product specificities in CDs synthesis by CGTases [16–18]. For instance, α-CD (91 % of ratio in total products) was obtained by addition of decanol, and β-CD (64 % of ratio in total products) was obtained by addition of cyclohexane [17]. Additionally, in the flavone glycosylation process by CGTases, OSs are necessary for the dissolution of most hydrophobic substrates (e.g., genistein [10,19], hesperidin [20,21], and naringin [22]). However, most OSs result in deactivation or dramatic drop in CGTases activity, thus improving the OSs resistance of CGTases is urgently required in many applications.

Abbreviations: CGTase, cyclodextrin glycosyltransferase; OS, organic solvent; CD, cyclodextrin; SASA, solvent accessible surface area; DMSO, dimethyl sulfoxide; MD, molecular dynamics.

* Corresponding authors.
E-mail addresses: hanrz@jiangnan.edu.cn (R. Han), u.schwaneberg@biotec.rwth-aachen.de (U. Schwaneberg).

[1] These two authors contributed equally to this work.

https://doi.org/10.1016/j.mcat.2023.113613
Received 30 August 2023; Received in revised form 1 October 2023; Accepted 7 October 2023
Available online 10 October 2023

Generally, following strategies [23] are commonly used for improving OS resistance of biocatalysts: (i) exploration of novel enzymes with OSs resistance [24–26]; (ii) process optimization of enzymatic reaction in presentence of OSs [27]; (iii) modification of enzymes for enhanced solvent resistance (including chemical modification [28], covalent cross-linking [29], immobilization [30,31], and directed evolution [32]). In addition, structure analysis reveals that solvent accessible surface area (SASA) [33], surface hydration [34], and surface charge [34] are important factors for OSs-resistant enzymes.

In our previous work, CGTase from *Paenibacillus macerans* (*Pm*CGTase) was engineered to improve its product specificity toward long chain glycosylated sophoricoside [10,19]. However, in the process of sophoricoside glycosylation, additional dimethyl sulfoxide (DMSO, cosolvent of sophoricoside) severely inhibited the activity of *Pm*CGTase.

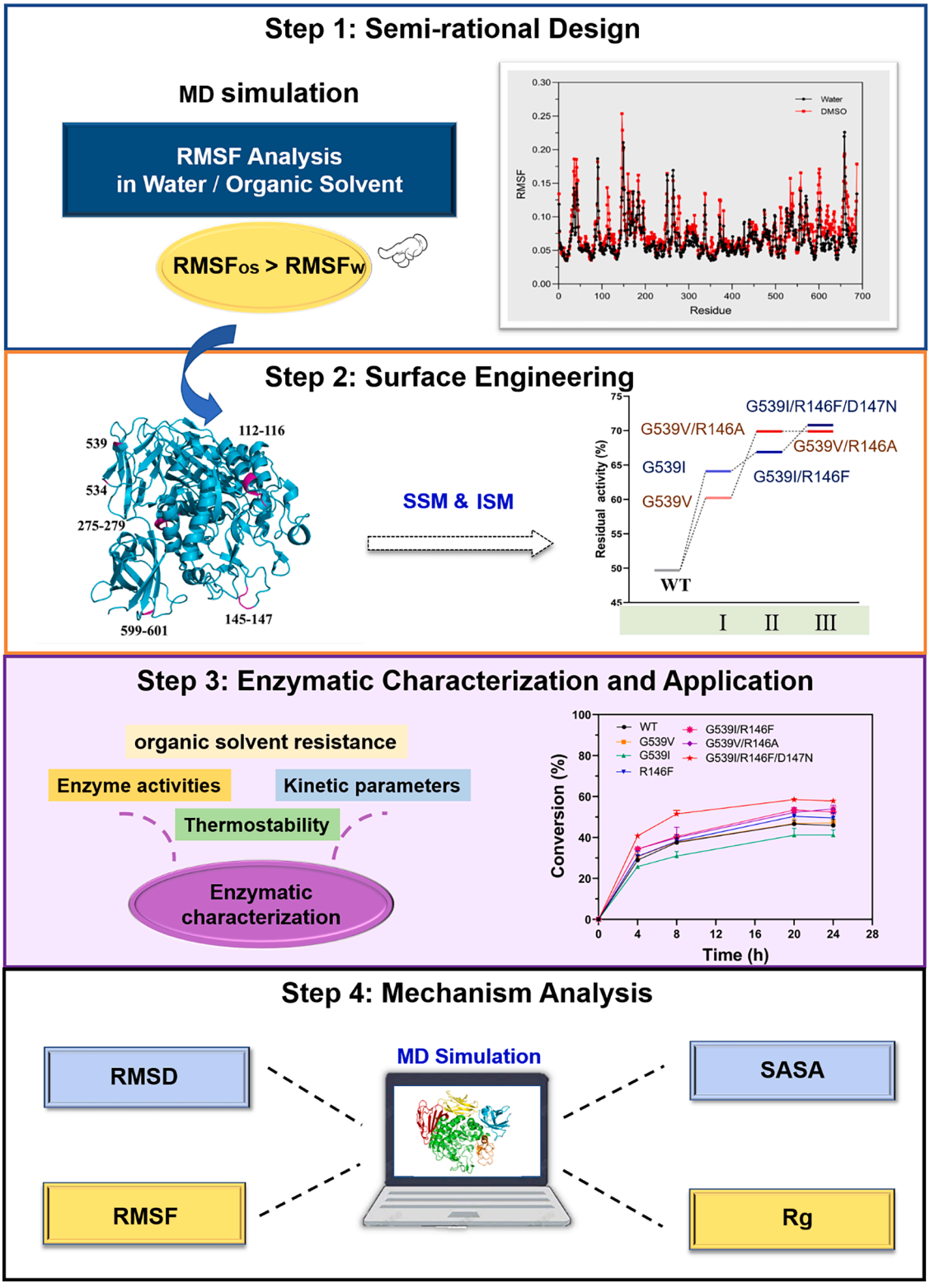

Fig. 1. Workflow of the engineering strategy in this study.

Up to now, few engineering strategy has been reported for the OSs-resistant CGTases. To improve the OSs resistance of *Pm*CGTase, herein semi-rational design guided by molecular dynamics (MD) simulation, and surface engineering strategies based on site saturation mutagenesis (SSM) and iterative saturation mutagenesis (ISM) [35] were adopted (Fig. 1). The best variant G539I/R146F/D147N with enhanced OSs resistance and thermostability was characterized. Finally, variant G539I/R146F/D147N was applied in the glycosylation of sophoricoside and its OSs-resistant mechanism was further explored. Our investigations not only reveal the mechanism of solvent resistance for *Pm*CGTase for the first time, but also provide important strategies for engineering solvent resistance of other related enzymes.

Experimental

Bacterial strains, plasmids, and chemicals

The *Pm*CGTase gene after systematic codon optimization was amplified by PCR from the plasmid pET20b (+)/*α-cgt* (GenBank accession no. JX412224) in our laboratory [36], then ligated into pET28a (+) plasmid to construct recombinant plasmid pET28a/*α-cgt* (wild-type). Subsequently, plasmid pET28a/*α-cgt* was transformed into the *E. coli* BL21 (DE3) competent cells (purchased from Novagen) for expression. KOD DNA polymerase was purchased from Shanghai Takara Co. Ltd. Soluble starch, sophoricoside, and maltodextrin were purchased from Shanghai Sangon Biotech. All other chemicals used were reagent grade products from Chinese reagent companies.

SSM and high-throughput screening (HTS) method

SSM of *Pm*CGTase was performed by whole plasmid PCR using KOD DNA polymerase with pET28a/*α-cgt* as a template. Primers were designed as listed in Table S1. The PCR was carried out in a Bio-Rad thermal cycler as follows: 94 °C for 5 min; 25 cycles consisting of 98 °C for 10 s, 50 °C for 30 s, and 68 °C for 4 min; 68 °C for 10 min. After digested with *Dpn* I, the PCR product was transferred into *E. coli* BL21 (DE3) competent cells, and incubated on LB agar plates (containing 50 μg/mL kanamycin) overnight.

The HTS method was developed from the previous report [37] with an appropriate modification. Single colony was inoculated in a sterile 96-deep well plate containing 300 μL LB medium with 50 μg/mL kanamycin each well, and cultured in shaker at 37 °C, 200 rpm overnight. After that, 100 μL of the overnight incubated culture was transferred to another 96-deep well plate containing 600 μL of TB medium with 50 μg/mL kanamycin, which was then incubated at 37 °C, 200 rpm in a shaker. When OD_{600} reached 0.6–0.8, IPTG was added with a final concentration of 0.05 mM for induction at 16 °C for 18 h.

After cultivation, the cells were collected by centrifugation at 4000 × g for 20 min, then disrupted with lysozyme (7000 U/mL) at 37 °C for 1 h. After centrifugation at 4 °C, 4000 × g for 10 min, 100 μL of supernatant was transferred to a pre-cooled 96-well plate, and equal volume of PBS buffer (pH 6.0) with or without appropriate concentration of DMSO was added. After stationary incubation at 4 °C for 1 h, 50 μL of maltodextrin (4 %, w/v) was added and incubated at 40 °C for 10 min. Then 250 μL of HCl (1 M) was immediately added to terminate the reaction, subsequently 150 μL of methyl orange (0.5 mM) was added. The solution was mixed evenly and stationarily incubated at room temperature for 20 min. Finally, the absorbance at 505 nm was measured. One unit of enzyme activity is defined as the amount of enzyme required to generate 1 μmol of α-cyclodextrin per minute. The group without DMSO is defined as the original activity, and the ratio of activities (group with DMSO/group without DMSO) is defined as the residual activity. Variants with 20 % higher residual activity than WT were screened as beneficial variants.

Z-factor reliability assessment of HTS method

Z-factor is the most widely used parameter in the evaluation and validation of HTS method [38]. The calculation formula is as follows:

$$Z = 1 - \frac{3\ \text{SD of sample} + 3\ \text{SD of control}}{|\ \text{mean of sample} - \text{mean of control}\ |}$$

The sample signal refers to the signal of the detected substance, while the control refers to the signal generated by the background interference factor. SD means standard deviation. In this study, the detection signals of *Pm*CGTase (WT) and no-load pET28a (+) were samples and background controls, respectively.

Expression and purification of PmCGTase

The recombinant strain harboring plasmid pET28a/α-cgt was inoculated into Luria-Bertani (LB) medium containing 50 μg/mL kanamycin at 37 °C, 200 rpm on a rotary shaker overnight. The overnight incubated culture was then transferred into Terrific-Broth (TB) medium containing 50 μg/mL kanamycin at an inoculum 1 %, and continued to culture in a shaker at 37 °C until optical density at 600 nm (OD_{600}) of the culture reached 0.8–1.0, then added isopropyl β-D-1-thiogalactopyranoside (IPTG) with a final concentration of 0.05 mM to induce at 16 °C for 18–20 h.

After induction and expression, the cells were collected by centrifugation and re-suspended in buffer A (pH 7.4, 20 mM imidazole, 0.5 M NaCl, 20 mM PBS), then disrupted by ultrasonic disintegration. The crude enzyme solution was obtained by centrifugation at 4 °C, 8000 × g for 20 min, and the supernatant was purified by a Ni-NTA agarose column (Qiagen, Chatsworth, CA, USA) with buffer A and buffer B (pH 7.4, 500 mM imidazole, 0.5 M NaCl, 20 mM PBS). Followed by gradient elution with different imidazole concentrations, the eluate was collected. The purity of the target protein was verified by SDS-PAGE. The pure enzyme solution was obtained after desalting via ultrafiltration tube followed by re-suspension of the purified protein in 1 mL potassium phosphate buffer (50 mM, pH 6.0), and finally frozen in liquid nitrogen and stored at −80 °C.

Activity assay of PmCGTase

The cyclization activity of *Pm*CGTase was measured by methyl orange method [36] with a slight modification. The reaction system included 100 μL of diluted enzyme solution, 50 μL of maltodextrin solution (4 % (w/v), dissolved in 50 mM PBS buffer (pH 6.0)) and 100 μL PBS buffer (50 mM, pH 6.0). After incubation at 40 °C for 10 min, the reaction was terminated by addition of 1 M HCl (250 μL). Then 150 μL of methyl orange (0.5 mM) was added, and the absorbance was measured at 505 nm after incubation at room temperature for 20 min. PBS buffer solution was used to replace enzyme solution in blank control. One unit of enzyme activity is defined as the amount of enzyme required to generate 1 μmol of α-cyclodextrin per minute.

The disproportionation activity of *Pm*CGTase was determined as described previously [39]. First, 300 μL of 4-nitro--phenyl-α-D-maltoheptaoside-4–6-O-ethylidene (EPS, 4 mM, dissolved in PBS buffer) and 300 μL maltose (0.2 mM, dissolved in PBS buffer) were mixed, preheated at 50 °C for 10 min. Then, 100 μL diluted enzyme solution was added and incubated at 50 °C for another 10 min. The reaction was terminated with 50 μL HCl (3 M). After 5 min, 50 μL NaOH (3 M) was added to neutralize the mixture. 100 μL α-Glucosidase was added to the mixture and incubated in a water bath of 60 °C for 1 h. Then 100 μL Na_2CO_3 (1 M) was added to adjust pH to 8.0. Absorbance was measured at 400 nm. One unit of disproportionation activity is defined as the amount of enzyme converting 1 μmol of EPS per minute.

The hydrolytic activity of *Pm*CGTase was determined by DNS colorimetry with a slight modification. Firstly, 50 μL dilute enzyme was mixed with 200 μL soluble starch solution (1 %, w/v, dissolved in 0.2 M

sodium acetate buffer, pH 5.5) and incubated in a water bath of 50 °C for 10 min. Then 500 μL of DNS solution was added and heated in boiling water for 7 min, immediately cooled in an ice water bath. The absorbance of solution was measured at 540 nm after diluting in equal volume with water. A control without the addition of *Pm*CGTase was used in this work. One unit of hydrolysis activity is defined as the amount of enzyme producing 1 μmol of reducing sugar per minute.

The protein concentration was determined using the commercially available Bradford Protein Assay Kit. Bovine serum albumin was used as standard and absorbance was recorded at 595 nm.

Enzymatic properties of PmCGTase

Resistance of OSs

After incubation in various OSs (DMSO, methanol, ethanol, and acetone) with different concentrations (diluting with PBS (50 mM, pH 6.0) buffer) at 4 °C for 1 h, residual activities of purified WT and its variants were measured by methyl orange method, and activities of enzymes without organic reagents were used as the control.

Optimum temperature and thermostability characterization

To investigate the effect of temperature on enzyme activity, the cyclization activities of WT and its variants were measured at various temperatures (30, 40, 50, 60 and 70 °C) (5 min of pre-warming before measurement). The highest activity of *Pm*CGTase at different temperatures was considered to be 100 %.

The thermostabilities of WT and its variants were also investigated as follows. Purified WT and variants (0.4 mg/mL) were stationarily incubated at 40 or 50 °C for various time. After cooling for 5 min on ice, their cyclization activities were determined at 40 °C. The enzymatic activities without stationary incubation at 40 or 50 °C were defined as 100 %.

Kinetic analysis

The activities of WT and its variants were assayed with maltodextrin solutions in different concentrations of 2.5–80 g/L in PBS buffer (50 mM, pH 6.0) at 40 °C. The Michaelis–Menten constant (K_m) and maximum velocity for the reaction (V_{max}) were calculated by the Michaelis−Menten equation using Origin pro 8.6 software. The k_{cat} and k_{cat}/K_m were also calculated for WT and variants, and the results were compared.

Transglycosylation of sophoricoside

Transglycosylation of sophoricoside by *Pm*CGTase was performed as previously described [10] with a slight modification. 1 mL of reaction solution including 200 μL of sophoroside (1 g/L, dissolved in DMSO), 600 μL of soluble starch (40 g/L, dissolved in PBS buffer, 50 mM, pH 6.0), and 200 μL of diluted pure *Pm*CGTase (0.05 mg/mL) was incubated at 40 °C, 120 rpm in a shaker. Reaction was terminated by heating at 100 °C for 10 min. After centrifugation at 12,000 × g for 15 min, the supernatant was analyzed by high-performance liquid chromatography (HPLC). Conversion was defined as the proportion of the amount of consumed sophoricoside to the amount of initial sophoricoside [10].

HPLC were performed using a Diamonsil C18 column (250 mm × 4.6 mm, 5 μm). Mobile phase consisted of solution A (acetonitrile) and solution B (0.1 % (v/v) phosphoric acid in deionized water). Gradient evolution was performed at 30 °C with a flow rate of 0.8 mL/min by the following procedure: 15 % A, 0–2 min; 15 %–85 % A, 2–17 min; 85 % A, 17–22 min; 85 %–15 % A, 22–25 min. Detection wavelength was 254 nm, and injection volume was 10 μL.

MD simulation

MD simulation were carried out using GROMACS 5.1.4 package and parameters (temperature 313 K; ionic strength 0.05 M; pH 6.0). Water and other heteroatoms were removed to revise the protein structure file. The GROMOS96(54a7) force field was selected for the simulation *Pm*CGTase in aqueous and organic systems [40]. The protonation state of ionizable residues was defined by pKa calculation at pH 6.0 using ProteinPrepare. After placing the protein in a constructed 10 nm cube box model, the simulation systems were filled with water molecules and OS molecules to achieve the desired percentage of solvent according to the experimental conditions. The cationic Na^+ and anion Cl^- were used to neutralize the charge in the system to ensure the net charge of the system was zero. Then, energy was minimized using the steepest descent and conjugate gradient algorithms to avoid adverse interaction interference. Before the MD simulation, a 100 ps NVT ensemble was performed at 313 K, followed by 100 ps equilibration in the NPT ensemble with restricted the position of CGTase. Lastly, MD simulation was conducted at 313 K for 100 ns.

Homology modeling of variants was performed with the crystal structure of *Pm*CGase (PDB ID:4JCL, 99 % similarity with variants) as the template, followed by above MD simulations based on variants model.

Results

Investigation of OSs resistance of PmCGTase

To investigate the influence of OSs on the stability of *Pm*CGTase, crude *Pm*CGTase was incubated in different OSs (e.g., DMSO, acetone, methanol, ethanol) at a concentration of 10 % (v/v) for 1 h for residual activities analysis. As shown in Fig. S1, the activity of *Pm*CGTase decreased in presence of the above four OSs compared with that in water, suggesting the necessity of improving OSs resistance. For instance, *Pm*CGTase retained 70 % of original activity after incubating in DMSO, while only approximate 40 % of activity after treatment of acetone, methanol or ethanol. Herein, DMSO was selected as the initial screening solvent for further investigation.

To further investigate the influence of DMSO at various concentrations (0, 5 %, 10 %, 15 %, 20 %, 25 %), residual activities were detected at different timescales (1, 2, and 4 h). As shown in Fig. S2, the activity of *Pm*CGTase significantly decreased with the increasing DMSO concentration. For instance, residual activity decreased from 91.6 % (in 5 % DMSO) to 16.4 % (in 25 % DMSO) after incubation for 1 h. Moreover, the activity loss was further aggravated with increasing incubation time in DMSO. To reduce the screening error and shorten screening time, incubation in 15 % DMSO for 1 h (44.5 % residual activity of *Pm*CGTase) was selected as screening condition for *Pm*CGTase with enhanced OSs resistance.

Development of HTS method of PmCGTase

Generally, cyclodextrins produced from starch or maltodextrin by CGTase can absorb the color of methyl orange, which causes a decrease in absorbance at 505 nm compared with that without cyclodextrins. Herein, optimization was performed on the following aspects: enzyme dosage, methyl orange dosage, reaction time, and substrate concentration. As shown in Table S2, the highest enzyme activity of 0.350 U/mL was achieved at the following HTS method conditions. In reaction stage, the optimum crude enzyme volume was 100 μL, and the best reaction time was 10 min. In color stage, the optimum methyl orange volume was 150 μL.

Semi-rational design of PmCGTase based on MD simulation

In order to improve the DMSO resistance of *Pm*CGTase, potential hotspots of *Pm*CGTase were predicted based on MD simulation, which was performed using crystal structure of *Pm*CGTase (PDB ID: 4JCL) as the template in water and DMSO, respectively. As shown in Fig. S3, several residues in two different solvents showed significantly different Root mean square fluctuation (RMSF) values, indicating key roles of

these sites in *Pm*CGTase for DMSO resistance. Finally, 18 surface residues (F112, G113, D114, F115, A116, D145, R146, D147, N275, E276, S277, G278, M279, T534, G539, T599, N600, Y601) were selected for further engineering due to their high flexibility in DMSO (higher RMSF values in DMSO than water).

Engineering of PmCGTase by SSM and ISM

SSM was performed on the above 18 hot residues, and results were showed in Fig. S4. Besides 8 residues (G113, F115, A116, N275, E276, G278, M279, T534), SSM toward other 10 residues (F112, D114, D145, R146, D147, S277, G539, T599, N600, Y601) resulted in variants with >20 % enhanced residual activities compared with WT, which were regarded as potential positive variants. After further confirmation with purified variants, five single variants (G539I, G539V, R146S, T599F, and D147L) showed higher residual activities than WT (45.1 % of residual activity) (Fig. 2). In particular, variants G539I (62.0 % of residual activity) and G539V (60.8 % of residual activity) exhibited the highest DMSO resistance, and R146S showed slightly lower activity than G539V. Therefore, ISMs were performed toward R146 with G539I and G539V as templates, respectively. The best double variants G539I/R146F and G539V/R146A showed 72.6 % and 73.5 % residual activities, respectively (Fig. 2). Subsequently, using G539I/R146F and G539V/R146A as templates respectively, ISMs were further performed toward sites 147 and 599, respectively. Results showed that the triple variant G539I/R146F/D147N displayed the best DMSO resistance (remaining 78.4 % of residual activity) with G539I/R146F as the template (Fig. 2), whereas no improved variant was obtained with G539V/R146A as the template. Using variant G539I/R146F/D147N as the template, further ISM at site 599 showed no improved residual activity. Therefore, 5 beneficial variants (G539I, G539V, G539I/R146F, G539V/R146A, G539I/R146F/D147N) were investigated for further characterization.

Characterizations of PmCGTase WT and variants

Specific activities analysis

Five variants (G539I, G539V, G539I/R146F, G539V/R146A, G539I/R146F/D147N) were expressed and purified for further characterization. As shown in Fig. S5, SDS-PAGE results demonstrated similar soluble-expression level between variants and WT with molecular mass of 74 kDa. Then the specific activities toward cyclization, hydrolysis, and disproportionation (in water) of purified *Pm*CGTase variants and WT were determined. As shown in Table 1, compared with WT, besides the triple variant G539I/R146F/D147N with a slightly increased disproportionation activity (7.4 %), other variants showed decreased (40 %–50 %) disproportionation activities. In particular, the disproportionation activities of single variants G539I and G539V were 48.3 % and 38.1 % lower than that of WT, respectively. In addition, compared with WT, G539I showed 53.4 % increased hydrolytic activity, while that of G539V, G539V/R164A were decreased by 43.8 % and 73.3 %, respectively. There was no significant distinction in hydrolytic activity between G539I/R146F, G539I/R146F/D147N and WT. In aspect of cyclization, G539I/R146F/D147N showed 16.9 % increased activity, whereas other variants showed no significant distinction compared with WT.

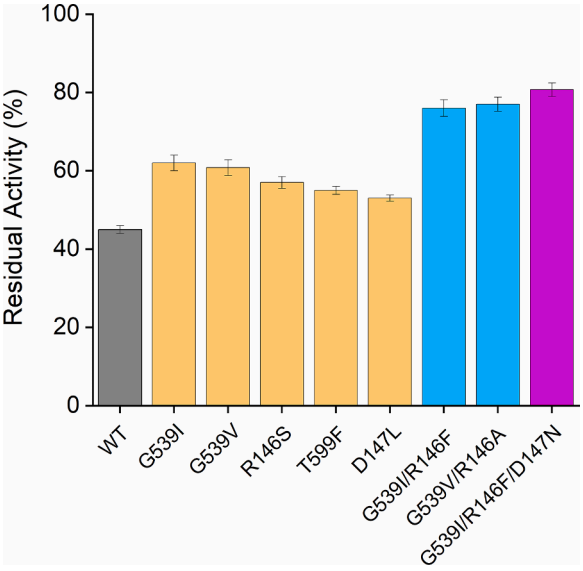

Fig. 2. Residual activity of purified beneficial variants of *Pm*CGTase. Before reaction, all purified enzymes were incubated at 15 % DMSO for 1 h, and their cyclization activities without incubation in 15 % DMSO were defined as 100 %. .

OSs resistance analysis

In order to investigate the OSs resistance of *Pm*CGTase variants, their residual activities in different OSs (DMSO, acetone, methanol, ethanol) were determined. As shown in Fig. 3A, all variants (especially for variants G539I/R146F/D147N and G539I/R146F) showed higher residual activities than WT in 10 %–30 % of DMSO, suggesting improved DMSO resistance of variants. For instance, the residual activity of best variant G539I/R146F/D147N was increased by 18.1 % (in 10 % DMSO)–79.4 % (in 30 % DMSO) compared with WT. Most variants displayed enhanced resistance toward acetone (except G539I, Fig. 3B), methanol (except G539I, Fig. 3C), and ethanol (Fig. 3D). Especially, compared with WT, the single variant G539V increased residual activity by 64 % (in 15 % acetone), 53.4 % (in 12 % methanol), and 59.2 % (in 12 % ethanol).

Thermostability

Herein, the optimum reaction temperature and thermostability of *Pm*CGTase WT and variants were investigated. As shown in Table 2, double/triple variants (G539I/R146F, G539V/R146A, and G539I/R146F/D147N) displayed the same optimum temperature as WT (50 °C), while single variants G539I and G539V showed lower optimum temperature (40 °C) than WT. The half-life ($t_{1/2}$) values of variants at 40 °C and 50 °C were also determined. As shown in Table 2, the $t_{1/2}$ value of variant G539V/R146A was 2.3-fold (at 40 °C) and 4.2-fold (at 50 °C) of that of WT (Table 2). In addition, compared with WT, the $t_{1/2}$ values of variant G539I/R146F increased by 97 % (at 40 °C) and 1.96-fold (at 50 °C), and that of G539I/R146F/D147N increased by 67 % (at 40 °C) and 63 % (at 50 °C) (Table 2). However, variants G539V and G539I showed poor thermostability at 40 °C, whose half-lives were less than half of WT (Table 2).

Kinetic analysis

Kinetic parameters of *Pm*CGTase variants in aqueous solution (PBS

Table 1
Specific activities of *Pm*CGTase and its variants.

	Disproportionation activity/(U/mg)	Hydrolysis activity/ ($\times 10^{-2}$ U/mg)	Cyclization activity/(U/mg)
WT	299.8 ± 8.5	14.6 ± 0.6	23.6 ± 3.1
G539I	154.9 ± 0.6	22.4 ± 2.2	21.9 ± 1.5
G539V	185.7 ± 2.2	8.2 ± 0.6	22.2 ± 0.9
G539I/R146F	240.7 ± 4.6	14.0 ± 1.4	23.8 ± 0.8
G539V/R146A	225.3 ± 3.2	3.9 ± 0.6	24.8 ± 0.6
G539I/R146F/D147N	322.1 ± 0.7	14.5 ± 0.8	27.6 ± 1.6

The value represents the mean of three independent experiments for each variant.

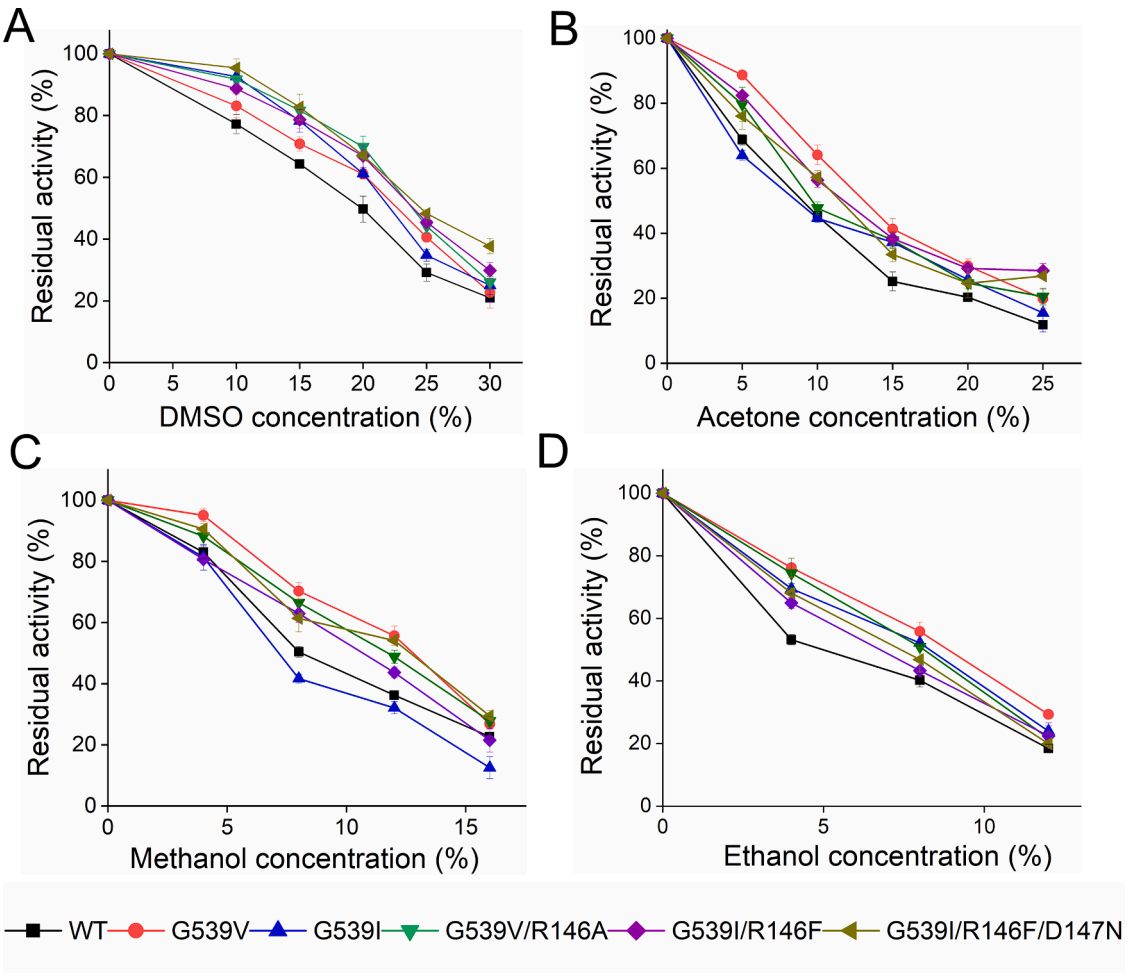

Fig. 3. Residual activity of purified *Pm*CGTase variants relative to WT after incubation in the varied concentration of (A) DMSO, (B) acetone, (C)methanol, and (D) ethanol. All data shown are average values from measurements in triplicates or more.

Table 2
Thermostability of *Pm*CGTase and its variants.

Enzymes	[a]Topt / °C	[b]$t_{1/2}$ / h (40 °C)	$t_{1/2}$ / min (50 °C)
WT	50	15.3 ± 0.2	33.2 ± 3.5
G539I	40	4.2 ± 0.1	35.5 ± 5.8
G539V	40	7.6 ± 0.2	39.8 ± 4.2
G539V/R146A	50	34.5 ± 0.3	140.9 ± 8.5
G539I/R146F	50	30.2 ± 0.3	98.5 ± 5.3
G539I/R146F/D147N	50	25.5 ± 0.3	54.3 ± 4.9

[a] T_{opt} means the optimum temperature.
[b] $t_{1/2}$ means the half-life of *Pm*CGTase and variants. The value represents the mean of three independent experiments for each variant.

buffer, pH 6.0) and OS system (15 % DMSO) were also determined at various concentrations of maltodextrin substrate (2.5–80 g/L). As shown in Table 3, except variant G539I/R146F/D147N with slightly lower K_m value, other variants showed higher K_m values than WT in water. However, all variants displayed lower K_m values than WT in 15 % DMSO, suggesting improved affinity of variants toward substrate in DMSO. Furthermore, increased k_{cat} values of variants led to increased k_{cat}/K_m values compared with WT both in water and DMSO (Table 3), suggesting improved catalytic efficiency of variants. For instance, compared with WT, the catalytic efficiency of variant G539I/R146F/D147N increased by 26.1 % in water and 41.9 % in DMSO.

Table 3
Kinetic analysis of *Pm*CGTase and its variants.

Enzymes	K_m (g L^{-1})		k_{cat} (× 10^2 min^{-1})		k_{cat}/K_m (L g^{-1} min^{-1})	
	Water	15 % DMSO	Water	15 % DMSO	Water	15 % DMSO
WT	17.4 ± 1.5	14.6 ± 0.7	14.3 ± 0.5	7.8 ± 0.2	82.7	53.4
G539I	24.3 ± 0.9	12.0 ± 0.6	17.6 ± 0.4	8.3 ± 0.2	72.4	69.2
G539V	23.0 ± 1.3	11.8 ± 0.8	16.8 ± 0.5	8.5 ± 0.3	73.0	72.0
G539V/ R146A	19.2 ± 0.9	10.9 ± 0.8	17.7 ± 0.4	9.2 ± 0.1	92.2	84.4
G539I/ R146F	23.6 ± 1.2	12.8 ± 0.7	19.2 ± 0.8	9.3 ± 0.2	81.4	72.7
G539I/ R146F/ D147N	16.2 ± 1.1	12.0 ± 0.7	16.9 ± 0.5	9.1 ± 0.2	104.3	75.8

Kinetic parameters were determined by methyl orange assay at different concentrations (2.5, 5, 10, 20, 25, 40, 50 and 80 g/L) of soluble starch, and all data shown are average values from measurements in triplicates or more.

Application of sophoricoside glycosylation using PmCGTase variants

Commonly, CGTases can catalyze the glycosylation of many hydrophobic substrates, such as genistin [11], sophoricoside [10], naringin [41], and Pueraria [42], which need to be solubilized by addition of OSs.

Herein, the *Pm*CGTase WT and variants were employed in the glycosylation of sophoricoside in 20 % DMSO (Fig. 4A). As shown in Fig. 4B, the reaction basically reached equilibrium after 20 h. Compared with WT (46.6 % of conversion), variants G539V/R146A, G539I/R146F and G539I/R146F/D147N gave increased conversions by 17.7 %, 14.3 % and 26.2 % respectively. However, Compared with WT, the single variants G539I and G539V showed similar and 5.5 % lower conversion, respectively.

Discussion

OSs play important roles in solubilizing hydrophobic substrates [20] and improving product specificity [16] in CGTases catalyzed reactions. However, native CGTases usually suffer from low activity in presence of OSs, constraining their industrial applications. Herein, *Pm*CGTase showed varied sensitivities toward different OSs (e.g., DMSO, acetone, methanol, ethanol) (Fig. S1). To enhance the OSs resistance of *Pm*CGTase, DMSO was selected as an initial screening solvent due to its lower evaporation and lower loss on *Pm*CGTase activity than other solvents (e.g., acetone, methanol, ethanol) (Fig. S1). An essential for a successful protein engineering campaign is reliable and robust screening system [43], herein the HTS method of CGTase was also developed. Based on results of preliminary experiments, *Pm*CGTase WT incubated in 15 % DMSO for 1 h with 44.5 % of residual activity (Fig. S2) was used as the control, leading to less error in screening process for positive variants. To evaluate the feasibility of the HTS method, Z-factor was calculated as to be 0.6 under the above optimum conditions (Table S3), which is regarded as a credible method ($0.5 \leq Z < 1$) [38].

Eighteen hot residues of *Pm*CGTase with higher RMSF values in DMSO than in water were selected based on MD analysis due to their higher flexibility in presence of OS, then 5 beneficial variants (G539I, G539V, G539I/R146F, G539V/R146A, G539I/R146F/D147N) were obtained after further engineering by SSM and ISM. Moreover, all these key residues are located at the enzyme surface, indicating important roles of surface residues on solvent stability of *Pm*CGTase, which is consistent with the results of reported lipases [23,40]. Subsequently, characterizations of these variants were analyzed. Compared with WT, all single and double variants (G539I, G539V, G539I/R146F and G539V/R146A) showed decreased disproportionation activities (Table 1). However, after the introduction of D147N, the disproportionation activity of G539I/R146F/D147N increased by 7.4 % compared with that of WT, suggesting the key role of the 147 residue for disproportionation. G539V and G539V/R146A showed significantly decreased hydrolytic activities compared with WT (Table 1), suggesting key inhibition on hydrolysis by substitution of glycine by valine at 539 site, although its location is far from the catalytic center of *Pm*CGTase. However, the triple variant G539I/R146F/D147N showed no significant distinction in all activities (disproportionation, hydrolysis and cyclodextrin) compared with WT, suggesting the synergy of the 3 residues (G539I, R146F, and D147N) has little effect on the catalytic center of *Pm*CGTase. Interesting, all *Pm*CGTase variants showed higher residual activities than WT in different OSs (Fig. 3), suggesting universally enhanced resistance of *Pm*CGTase variants toward most OSs, which was consistent with the conclusion of reported *Bacillus subtilis* lipase A (BSLA) [33,34]. However, these variants showed different resistant-capacity to different OSs. For instance, the triple variant G539I/R146F/D147N showed the best resistance to DMSO, while single variant G539V showed the best resistance to acetone, methanol and ethanol (Fig. 3). In addition, compared with DMSO, *Pm*CGTase and variants were more sensitive to acetone, methanol and ethanol, which may be attributed to their different polarity. Moreover, compared with WT, variants showed enhanced affinity toward substrate and improved catalytic efficiency in DMSO (Table 3), which may be attributed to their enhanced OSs resistance.

As one of the important indicators of biocatalysts in industrial applications, thermostability is usually positively correlated with solvent tolerance [40]. Herein, compared with WT, except single variants (G539V and G539I), double/triple variants (G539I/R146F, G539V/R146A, and G539I/R146F/D147N) exhibited enhanced thermostability at 40 °C and 50 °C (Table 2), suggesting that the 146 residue may play an important role in the thermostability of *Pm*CGTase. In the glycosylation of sophoricoside in 20 % DMSO at 40 °C by *Pm*CGTase WT and variants, enhanced conversion by double and triple variants (G539V/R146A, G539I/R146F and G539I/R146F/D147N) may be attributed to their enhanced resistance to DMSO and thermostability. Although single variants G539I and G539V also showed improved DMSO resistance, their glycosylation conversions were not enhanced compared with WT, which may be ascribed to their decreased

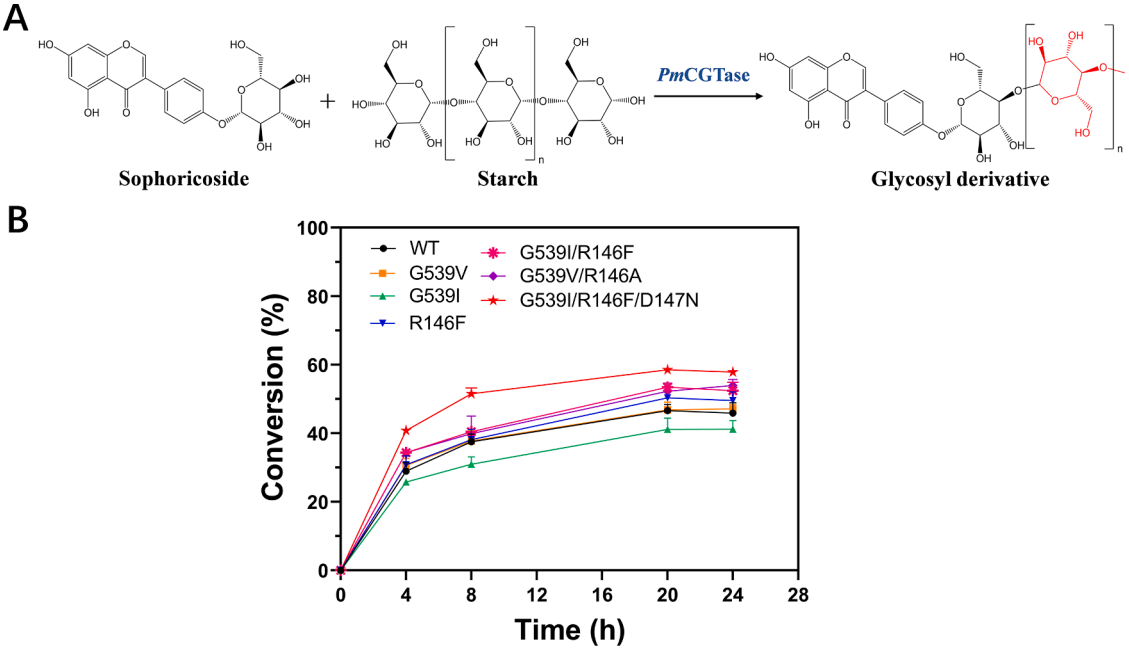

Fig. 4. (A) Glycosylation reaction of sophoricoside. (B) Time course of sophoricoside catalyzed by WT *Pm*CGTase and its variants.

disproportionation activities and poor thermostability.

To gain insight into the mechanism of the OS-resistant variants, MD simulations of the best variant G539I/R146F/D147N and WT in the presence of 20 % DMSO or water were performed. Root mean square deviation (RMSD), as a common indicator of the structural stability, was calculated based on MD simulation (Fig. 5A). In water, the RMSD curves showed a similar trend between WT and variant G539I/R146F/D147N. In 20 % DMSO, the average RMSD value of variant G539I/R146F/D147N remained at 0.15 nm, significantly lower than that of WT (0.19 nm) (Fig. 5B), indicating a more stable protein skeleton of the variant. Previous reports also confirmed that enzymes with lower RMSD values tended to be higher resistance toward OSs [44]. Radius of gyration (Rg) is also an important index to evaluate the overall structural compactness of enzyme [45]. Herein, Rg values of variant G539I/R146F/D147N and WT between in water and in DMSO were also calculated (Fig. 5C and D). Slightly higher Rg value of WT than that of variant in DMSO (Fig. 5D) indicates that the structure of the variant is tighter than that of WT, which may be conducive to the enhanced resistance of OSs and thermostability.

RMSF value represents the fluctuation of each residue, which is an indicator of freedom of atomic motion and represents the flexibility of molecular structure [45]. RMSF values of residues (I539, F146, N147) in the triple variant G539I/R146F/D147N was lower than that of residues (G539, R146, D147) in WT both in water and 20 % DMSO (Fig. 6A and B), revealing enhanced local structural rigidity of the variant and its strengthened stability in OSs.

Some enzymes (e.g., BSLA) with increased surface hydration was regarded as an important factor for enhanced OSs resistance [34]. However, herein the number of water molecules around three substituted residues slightly decreased in variant G539I/R146F/D147N compared with WT (Fig. S6), which may be attributed to the polarity of residues on the surface. Compared with WT, substituted residues of G539I, R146F and D147N contribute to increased hydrophobicity, leading to decreased number of surface bound water of the variant. Moreover, similar activities of WT and variant G539I/R146F/D147N (Table 1) indicate that the slightly decreased number of water molecules in the variant would not destroy the structure of *Pm*CGTase.

SASA is also an important data for the stability analysis of enzymes in solvents. Generally, an increased SASA value is often caused by denaturation of protein to expose more surface area [46]. Herein, SASA values of the residues at the 146, 147, and 539 sites of WT and the variant were calculated in water and DMSO conditions, respectively. As shown in Fig. 6C and D, residues at 147 and 539 sites both in water and DMSO showed similar SASA values. However, R146 (WT) showed higher SASA value in DMSO than in water (Fig. 6C), while F146 (variant) displayed lower SASA value in DMSO than in water (Fig. 6D). Therefore, residues at R146 site may play an important role in the structure stability of variant, which is also consistent with the results of increased thermostability of variant of G539V/R146A and G539I/R146F (Table 2).

Conclusion

In conclusion, OSs resistance is important for CGTases in glycosylation of hydrophobic phenolic compounds. In this study, MD simulation guided identification of potential residues and surface engineering were proved to be efficient strategies for enhanced OSs resistance of *Pm*CGTase. The best variant G539I/R146F/D147N with significantly enhanced OSs resistance (e.g., DMSO, acetone, methanol, ethanol) and thermostability was successfully obtained, with 41.9 % higher catalytic efficiency (k_{cat}/K_m value) than WT in 15 % DMSO. Furthermore, compared with WT, the glycosylation efficiency of sophoricoside by G539I/R146F/D147N was increased by 26.2 % in 20 % DMSO. Finally, in depth computational analysis based on MD simulation indicates that the strengthened local structural rigidity and compactness is mainly responsible for the enhanced OSs resistance. This semi-rational engineering strategy could provide guidance for engineering OSs resistance of other glycosyltransferases and hydrolases, therefore broaden their

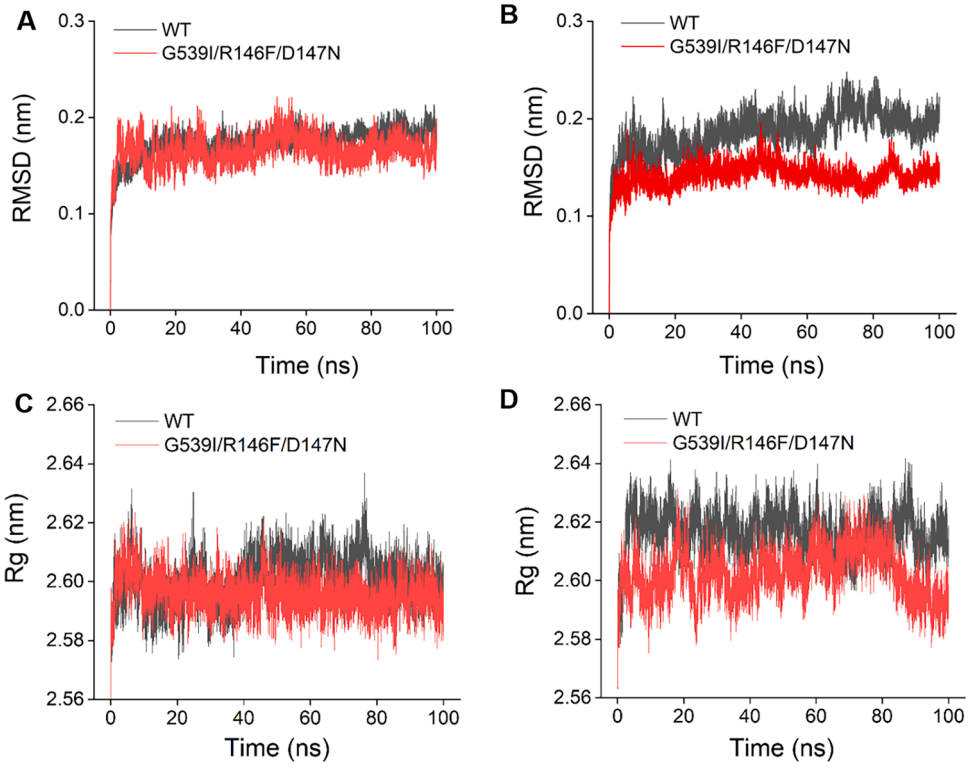

Fig. 5. Comparison of MD simulations of WT *Pm*CGTase and the best variant G539I/R146F/D147N. (A) RMSD in water; (B) RMSD in DMSO; (C) Rg in water; (D) Rg in DMSO;.

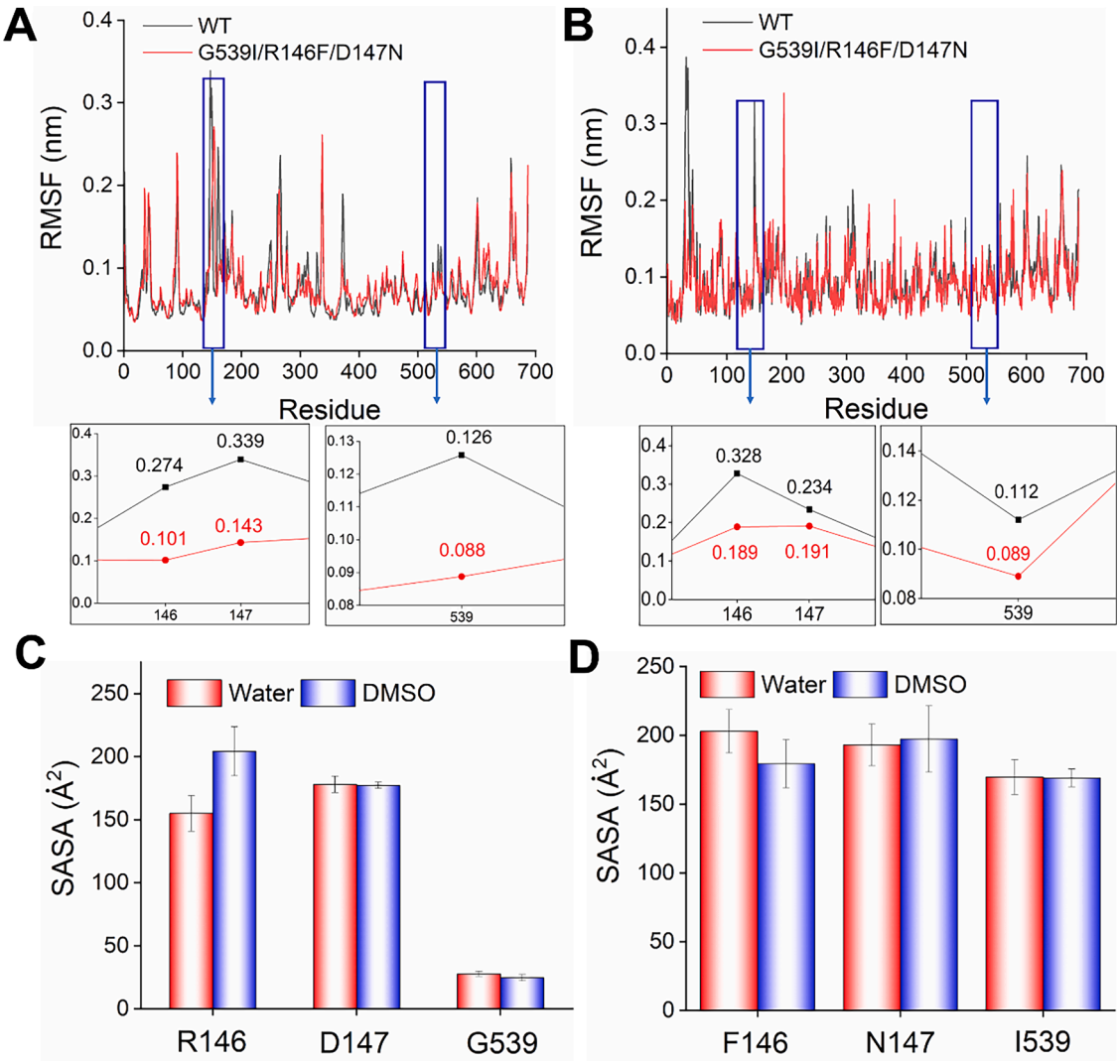

Fig. 6. Comparison of RMSF and SASA of WT *Pm*CGTase and the variant G539I/R146F/D147N (A) RMSF in water; (B) RMSF in DMSO; (C) SASA of WT; (D) SASA of G539I/R146F/D147N.

industrial application.

CRediT authorship contribution statement

Ruizhi Han: Formal analysis, Writing – original draft, Funding acquisition, Supervision. **Yulin Jiang:** Formal analysis, Writing – original draft, Data curation, Methodology, Software. **Siyan Liu:** Data curation, Methodology, Software. **Yu Ji:** Writing – review & editing, Validation. **Ulrich Schwaneberg:** Writing – review & editing, Validation. **Ye Ni:** Funding acquisition, Supervision.

Declaration of Competing Interest

The authors have declared that there are no conflicts of interest.

Data availability

Data will be made available on request.

Acknowledgments

This work was supported by the National Key Research and Development Program of China (2021YFC2102700), the National Natural Science Foundation of China (31871738, 22077054), the National First-Class Discipline Program of Light Industry Technology and Engineering (LITE2018-07), the Program of Introducing Talents of Discipline to Universities (111-2-06).

Supplementary materials

Supplementary material associated with this article can be found, in the online version, at doi:10.1016/j.mcat.2023.113613.

References

[1] J.D. Schoffer, M.P. Klein, R.C. Rodrigues, P.F. Hertz, Continuous production of beta-cyclodextrin from starch by highly stable cyclodextrin glycosyltransferase immobilized on chitosan, Carbohydr. Polym. 98 (2013) 1311–1316.
[2] Z.F. Li, M. Wang, F. Wang, Z.B. Gu, G.C. Du, J. Wu, J. Chen, γ-Cyclodextrin: a review on enzymatic production and applications, Appl. Microbiol. Biotechnol. 77 (2007) 245–255.
[3] B.A. vander Veen, J.C.M. Uitdehaag, B.W. Dijkstra, L. Dijkhuizen, Engineering of cyclodextrin glycosyltransferase reaction and product specificity, Biochim. Biophys. Acta. 1543 (2000) 336–360.
[4] H.Y. Ji, Y.X. Bai, Y.X. Liu, Y.L. Wang, X.B. Zhan, J. Long, L. Chen, C. Qiu, Z.Y. Jin, Deciphering external chain length and cyclodextrin production with starch catalyzed by cyclodextrin glycosyltransferase, Carbohydr. Polym. 284 (2022), 119156.

[5] M. Huang, C.M. Li, Z.B. Gu, L. Cheng, Y. Hong, Z.F. Li, Mutations in cyclodextrin glycosyltransferase from *Bacillus circulans* enhance beta-cyclization activity and beta-cyclodextrin production, J. Agric. Food Chem. 62 (2014) 11209–11214.
[6] N. Szerman, I. Schroh, A.L. Rossi, A.M. Rosso, N. Krymkiewicz, S.A. Ferrarotti, Cyclodextrin production by cyclodextrin glycosyltransferase from *Bacillus circulans* DF 9R, Bioresour. Technol. 98 (2007) 2886–2891.
[7] B.N. Gawande, A.Y. Patkar, Purification and properties of a novel raw starch degrading-cyclodextrin glycosyltransferase from *Klebsiella pneumoniae* AS-22, Enzyme. Microb. Technol. 28 (2001) 735–743.
[8] X.M. Tao, L.Q. Su, S. Chen, L. Wang, J. Wu, Producing 2-O-D-glucopyranosyl-L-ascorbic acid by modified cyclodextrin glucosyltransferase and isoamylase, Appl. Microbiol. Biotechnol. 107 (2023) 1233–1241.
[9] X.M. Tao, D.M. Kong, H.H. Zhang, L.Q. Su, S. Chen, D.M. Rao, B.B. Wei, J. Wu, L. Wang, Enhancing 2-O-alpha-D-glucopyranosyl-L-ascorbic acid synthesis by weaking the acceptor specificity of CGTase toward glucose and maltose, Bioproc. Biosyst. Eng. 46 (2023) 903–911.
[10] R.Z. Han, J. Ni, J.Y. Zhou, J.J. Dong, G.C. Xu, Y. Ni, Engineering of cyclodextrin glycosyltransferase reveals pH-regulated mechanism of enhanced long-chain glycosylated sophoricoside specificity, Appl. Environ. Microbiol. 86 (2020) e00004–e00020.
[11] D. Li, S.A. Roh, J.H. Shim, B. Mikami, M.Y. Baik, C.S. Park, K.H. Park, Glycosylation of genistin into soluble inclusion complex form of cyclic glucans by enzymatic modification, J. Agric. Food. Chem. 53 (2005) 6516–6524.
[12] J.L. Gonzalez-Alfonso, A. Poveda, M. Arribas, Y. Hirose, M. Fernandez-Lobato, A. O. Ballesteros, J. Jimenez-Barbero, F.J. Plou, Polyglucosylation of rutin catalyzed by cyclodextrin glucanotransferase from *Geobacillus* sp.: optimization and chemical characterization of products, Ind. Eng. Chem. Res. 60 (2021) 18651–18659.
[13] Y.H. Go, T.K. Kim, K.W. Lee, Y.H. Lee, Functional characteristics of cyclodextrin glucanotransferase from *Alkalophilic Bacillus sp.* BL-31 highly specific for intermolecular transglycosylation of bioflavonoids, J. Microbiol. Biotechnol. 17 (2007) 1550–1553.
[14] X.J. Yu, J.S. Yang, B.Z. Li, H.L. Yuan, High efficiency transformation of stevioside into a single mono-glycosylated product using a cyclodextrin glucanotransferase from *Paenibacillus sp*. CGMCC 5316, World J. Microbiol. Biotechnol. 31 (2015) 1983–1991.
[15] S. Li, W. Li, Q.Y. Xiao, Y.M. Xia, Transglycosylation of stevioside to improve the edulcorant quality by lower substitution using cornstarch hydrolyzate and CGTase, Food Chem. 138 (2013) 2064–2069.
[16] B.T. Tesfai, D. Wu, S. Chen, J. Chen, J. Wu, Effect of organic solvents on the yield and specificity of cyclodextrins by recombinant cyclodextrin glucanotransferase (CGTase) from *Anaerobranca gottschalkii*, J. Incl. Phenom. Macro. 77 (2013) 147–153.
[17] A.D. Blackwood, C. Bucke, Addition of polar organic solvents can improve the product selectivity of cyclodextrin glycosyltransferase-Solvent effects on CGTase, Enzyme Microb. Technol. 27 (2000) 704–708.
[18] A. Biwer, G. Antranikian, E. Heinzle, Enzymatic production of cyclodextrins, Appl. Microbiol. Biotechnol. 59 (2002) 609–617.
[19] R.Z. Han, B.C. Chai, Y.L. Jiang, J. Ni, Y. Ni, Engineering of cyclodextrin glycosyltransferase from *Paenibacillus macerans* for enhanced product specificity of long-chain glycosylated sophoricosides, Mol. Catal. 519 (2022), 112147.
[20] S.S. Choi, S.H. Lee, K.A. Lee, A comparative study of hesperetin, hesperidin and hesperidin glucoside: antioxidant, anti-inflammatory, and antibacterial activities in vitro, Antioxidants 11 (2022) 1618.
[21] M. Yamada, F. Tanabe, N. Arai, H. Mitsuzumi, Y. Miwa, M. Kubota, H. Chaen, M. Kibata, Bioavailability of glucosyl hesperidin in rats, Biosci. Biotechnol. Biochem. 70 (2006) 1386–1394.
[22] S.J. Lee, J.C. Kim, M.J. Kim, M. Kitaoka, C.S. Park, S.Y. Lee, M.J. Ra, T.W. Moon, J. F. Robyt, K.H. Park, Transglycosylation of naringin by *Bacillus stearothermophilus* maltogenic amylase to give glycosylated naringin, J. Agric. Food. Chem. 47 (1999) 3669–3674.
[23] N. Doukyu, H. Ogino, Organic solvent-tolerant enzymes, Biochem. Eng. J. 48 (2010) 270–282.
[24] N. Doukyu, H. Kuwahara, R. Aono, Isolation of *Paenibacillus illinoisensis* that produces cyclodextrin glucanotransferase resistant to organic solvents, Biosci. Biotechnol. Biochem. 67 (2003) 334–340.
[25] N. Akbari, S. Daneshjoo, J. Akbari, K. Khajeh, Isolation, characterization, and catalytic properties of a novel lipase which is activated in ionic liquids and organic solvents, Appl. Biochem. Biotechnol. 165 (2011) 785–794.
[26] P. Anbu, B.K. Hur, Isolation of an organic solvent-tolerant bacterium *Bacillus licheniformis* PAL05 that is able to secrete solvent-stable lipase, Biotechnol. Appl. Biochem. 61 (2014) 528–534.
[27] M. Szczesna-Antczak, A. Kubiak, T. Antczak, S. Bielecki, Enzymatic biodiesel synthesis-key factors affecting efficiency of the process, Renew. Energ. 34 (2009) 1185–1194.
[28] S. Kajiwara, K. Komatsu, R. Yamada, T. Matsumoto, M. Yasuda, H. Ogino, Modification of lipase from *Candida cylindracea* with dextran using the borane-pyridine complex to improve organic solvent stability, J. Biotechnol. 296 (2019) 1–6.
[29] S.H. Kim, S.J. Kim, S. Park, H.K. Kim, Biodiesel production using cross-linked *Staphylococcus haemolyticus* lipase immobilized on solid polymeric carriers, J. Mol. Catal. B.: Enzym. 85 (86) (2013) 10–16.
[30] T. Matsumoto, R. Yamada, H. Ogino, Chemical treatments for modification and immobilization to improve the solvent-stability of lipase, World J. Microbiol. Biotechnol. 35 (2019) 193.
[31] Z. Zhou, F. Piepenbreier, V.R.R. Marthala, K. Karbacher, M. Hartmann, Immobilization of lipase in cage-type mesoporous organosilicas via covalent bonding and crosslinking, Catal. Today 243 (2015) 173–183.
[32] J. Batra, S. Mishra, Organic solvent tolerance and thermostability of a beta-glucosidase co-engineered by random mutagenesis, J. Mol. Catal. B.-Enzym. 96 (2013) 61–66.
[33] H.Y. Cui, L.L. Zhang, L. Eltoukhy, Q.J. Jiang, S.K. Korkunc, K.E. Jaeger, U. Schwaneberg, M.D. Davari, Enzyme hydration determines resistance in organic cosolvents, ACS Catal. 10 (2020) 14847–14856.
[34] H.Y. Cui, M. Vedder, L.L. Zhang, K.E. Jaeger, U. Schwaneberg, M.D. Davari, Polar substitutions on the surface of a lipase substantially improve tolerance in organic solvents, ChemSusChem 15 (2022), e202102551.
[35] G. Qu, A. Li, C.G. Acevedo-Rocha, Z. Sun, M.T. Reetz, The crucial role of methodology development in directed evolution of selective enzymes, Angew. Chem. Int. Ed. 59 (2020) 13204–13231.
[36] Z.F. Li, B. Li, Z.B. Gu, G.C. Du, J. Wu, J. Chen, Extracellular expression and biochemical characterization of alpha-cyclodextrin glycosyltransferase from *Paenibacillus macerans*, Carbohydr. Res. 345 (2010) 886–892.
[37] X. Tao, L. Su, L. Wang, X. Chen, J. Wu, Improved prodution of cyclodextrin glycosyltransferase from *Bacillus stearothermophilus* NO2 in *Escherichia coli* via directed evolution, Appl. Microbiol. Biotechnol. 104 (2020) 173–185.
[38] N. Malo, J.A. Hanley, S. Cerquozzi, J. Pelletier, R. Nadon, Statistical practice in high-throughput screening data analysis, Nat. Biotechnol. 24 (2006) 167–175.
[39] B.A. van der Veen, G. van Alebeek, J.C.M. Uitdehaag, B.W. Dijkstra, L. Dijkhuizen, The three transglycosylation reactions catalyzed by cyclodextrin glycosyltransferase from *Bacillus circulans* (strain 251) proceed via different kinetic mechanisms, Eur. J. Biochem. 267 (2000) 658–665.
[40] H.Y. Cui, K.E. Jaeger, M.D. Davari, U. Schwaneberg, CompassR yields highly organic-solvent-tolerant enzymes through recombination of compatible substitutions, Chemistry (Easton) 27 (2021) 2789–2797.
[41] T. Kometani, T. Nishimura, T. Nakae, H. Takii, S. Okada, Synthesis of neohesperidin glycosides and naringin glycosides by cyclodextrin glucanotransferase from an *alkalophilic Bacillus species*, Biosci. Biotechnol. Biochem. 60 (2010) 645–649.
[42] W. Huang, Q. He, Z.R. Zhou, H.B. He, R.W. Jiang, Enzymatic synthesis of puerarin glucosides using cyclodextrin glucanotransferase with enhanced antiosteoporosis activity, ACS Omega 5 (2020) 12251–12258.
[43] A. Sarnaik, A. Liu, D. Nielsen, A.M. Varman, High-throughput screening for efficient microbial biotechnology, Curr. Opin. Biotechnol. 64 (2020) 141–150.
[44] Y.Y. Xia, W.W. Guo, L.C. Han, W. Shen, X.Z. Chen, H.Q. Yang, Significant improvement of both catalytic efficiency and stability of fructosyltransferase from *Aspergillus niger* by structure-guided engineering of key residues in the conserved sequence of the catalytic domain, J. Agric. Food. Chem. 70 (2022) 7202–7210.
[45] M. Mohtashami, J. Fooladi, A. Haddad-Mashadrizeh, M.R. Housaindokht, H. Monhemi, Molecular mechanism of enzyme tolerance against organic solvents: insights from molecular dynamics simulation, Int. J. Biol. Macromol. 122 (2019) 914–923.
[46] D.W. Zhang, R. Lazim, Application of conventional molecular dynamics simulation in evaluating the stability of apomyoglobin in urea solution, Sci. Rep. 7 (2017) 44651.